Materials Transactions, JIM, Vol. 41, No. 11 (2000) pp. 1427 to 1431
Special Issue on Bulk Amorphous, Nano-Crystalline and Nano-Quasicrystalline Alloys

The Effects of Iron Addition on the Glass-Forming Ability and Properties of Zr–Ti–Cu–Ni–Be–Fe Bulk Metallic Glass

De Qian Zhao, Yong Zhang, Ming Xiang Pan and Wei Hua Wang*

Institute of Physics and Center for Condensed Matter Physics, Chinese Academy of Sciences, Beijing 100080, P.R. China

Zr–Ti–Cu–Ni–Be–Fe bulk metallic glasses and metallic glassy matrix composites were produced by water quenching method. The effect of Fe addition on glass forming ability, hardness, magnetic susceptibility and thermal stability of the alloys was investigated. It was found that the glass forming ability and the properties of the alloys were sensitive to Fe content. A single amorphous phase was obtained in the alloys up to 8 at%Fe addition. These bulk metallic glasses exhibited high thermal stability, wide super-cooled liquid region, and anomalous magnetic susceptibility χ versus temperature in the supercooled liquid region. Metallic glassy composites consisting of nanocrystalline $FeZr_2$ particles were obtained in the alloys with more than 10 at%Fe addition.

(Received July 24, 2000; Accepted October 31, 2000)

Keywords: *bulk metallic glasses, glass-forming ability, iron addition, magnetic susceptibility*

1. Introduction

Recently, multicomponent bulk metallic glasses (BMGs) with an excellent glass-forming ability (GFA) and properties have attracted great interest of many researchers because of their promising engineering applications and scientific significance.[1–5] The Zr-based BMGs exhibit high tensile strength, good ductility, high elastic energy and impact fracture energy, and high corrosion resistance.[6] The Fe-based BMGs such as Fe–Al–Ga–P–B–C exhibit excellent soft magnetic properties.[7,8] It was found that the GFA, thermal stability and properties of the glass-forming alloys were sensitive to the addition of elements.[9–15] Be addition (the smallest metallic atom) is effective to increase the viscosity of the ZrTiCuNi alloy, the nucleation and growth of crystalline phases in the supercooled liquid region (SLR) are obstructed,[8–10] the $Zr_{41}Ti_{14}Cu_{12.5}Ni_{10}Be_{22.5}$ alloy is then of excellent GFA and can be formed with a critical cooling rate below 1 K/s. Gebert *et al.*[12] found that more than 0.5 at% oxygen in a glass-forming alloy led to the marked decrease of the GFA. Little carbon or silicon addition (about 1 at%) can enhance the thermal stability and mechanical properties of the Zr-based alloys.[13,14] Above results show that the addition of some special elements can markedly affect the GFA and the properties of a glass forming alloy. On the other hand, the addition method could be used to fabricate the composite with nanoscale particle in the glassy matrix through the addition-induced partial crystallization.[15] In this work, Fe is chosen as an additional element. It is well known that α-Fe is a ferromagnetic substance, so Fe contented BMGs hold the potential use of soft magnetic properties. On the other hand, iron is analogous element of Ni and relatively cheaper than other transition metals for the application of the BMGs as structural materials. The GFA of the Fe based BMGs such as FeAlGaPBC is not so good, the maximum 3-dimension size of this kind of BMG is only about 2 mm.[8] So the study of Fe contented BMGs is a practical way to explore the influence of the analogous elements on the GFA and the properties of a BMG. The effects of Fe on the formation and the properties of the $Zr_{41}Ti_{14}Cu_{12.5}Ni_{10}Be_{22.5}$ BMG were investigated. Fully BMG can be obtained with Fe adding up to 8 at%. The glassy matrix composites with nanocrystalline particle were obtained in the alloy with more than 8 at%Fe addition. An anomalous change of the magnetic susceptibility upon temperature in the SLR was observed.

2. Experiments

$Zr_{41-X}Ti_{14}Cu_{12.5}Ni_{10-Y}Be_{22.5-Z}Fe_{X+Y+Z}$ (X = 0–8, Y = 0–10, Z = 0–5) ingots were prepared by arc-melting a mixture of elements with purity up to 99.9% or better in Ti-gettered Ar atmosphere, the background vacuum is better than 10^{-3} Pa. The ingots were remelted in a vacuum sealed quartz tube and quenched in water to get amorphous rods with diameter of 8–16 mm, the details of the experimental procedure can be seen in Refs. 9–10). The diameter of the investigated samples in this work is 10 mm. The cross-sectional slices cut from the rod were used for structure and properties investigations. Structural characterization of the as-quenched samples has been done by using JEM-200CX transmission electron microscopy (TEM), Siemens D5000 X x-ray diffractometry (XRD) with a Cu K_α radiation. The thermal analysis was performed by differential scanning calorimetry (Perkin Elmer DSC-7) with a heating rate of 0.167 K/s. The melting temperature (solidus temperature) is measured by differential temperature analysis (DTA) with a heating rate of 0.167 K/s. The micro-hardness was measured with a Newphoto-21 micro-hardness tester at a load of 100 g. The magnetic susceptibility was measured by magnetic balance (MB-2), and the intensity of the magnetization was 1.2 T. The specimens were heated up to the desired temperature using a rate about 0.167 K/s to ensure the same thermal history for all specimens.

*Author to whom the correspondence should be addressed, E-mail: whw@aphy.iphy.ac.cn

3. Results and Discussions

Figure 1 exhibits XRD patterns of the Zr–Ti–Cu–Ni–Be–Fe alloys with different Fe content. Figures 1 (a) to (e) exhibit only a broad diffuse scattering peak characterizing amorphous nature of these alloys within the sensitivity limit of XRD. The result indicates that up to 8 at%Ni and 5 at%Zr can be replaced by Fe in the ZrTiCuNiBe alloy. Fe and Ni belong to the same transitional subgroup in elemental periodic table, the atomic radius and electronegativity of Fe are close to those of Ni. The GFA of the Zr–Ti–Cu–Ni–Be–Fe alloy is not significantly changed when substituting less than 8 at%Ni with Fe. At more than 10 at%Fe addition, sharper diffraction peaks superimpose on the broad diffuse scattering peak meaning a glassy matrix composite formation. The main crystalline phase identified according to the indexing scheme is $FeZr_2$. The average sizes of the crystalline grains, estimated by the Scherrer formula from the full width at half-maximum (FWHM) of the crystalline peaks, are 5 to 10 nm. From Figs. 1(f) to (i), it can be clearly seen that the crystalline peaks become weaker and broader with increasing Fe addition, this indicates that the average grain size of crystalline $FeZr_2$ decreases with increasing Fe addition. Figure 2 is TEM photograph of the as-quenched $Zr_{36}Ti_{14}Cu_{12.5}Ni_5Be_{20.5}Fe_{12}$ alloy. The TEM result confirms that the alloy is a composite consisting of nano-scale crystalline particles embedded in the glassy matrix. It is known that the multi-component glass-forming alloy can have a very high viscosity and extreme low atomic diffusion in the melt,[6,8] the properties inhibit the growth of the crystalline nuclei, and the nanoscale grains were then obtained. The crystalline $FeZr_2$ is the prior precipitation phase, because Fe and Zr have the largest negative heat mixing enthalpy (37 KJ/mol[16]) among the constitutes of the alloy.

DSC traces for the Zr–Ti–Cu–Ni–Be–Fe fully amorphous alloys are presented in Fig. 3. It can be seen that all DSC curves exhibit an endothermic characteristic of a glass transition followed by several exothermic crystallization peaks at higher temperature. T_g is defined as the onset glass transition temperature, T_{x1}, T_m and T_{rg} are the onset temperature of the first crystallization event, melting temperature and reduced glass transition temperature, respectively. $\Delta T = T_{x1} - T_g$ is referred to as the SLR. As shown in Fig. 3, all the BMGs

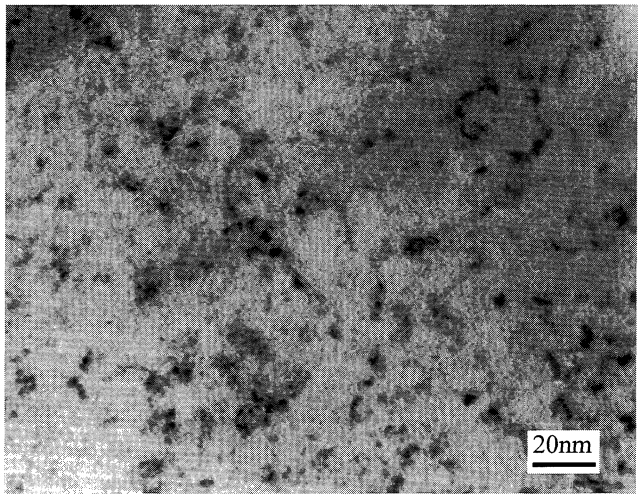

Fig. 2 TEM photograph of the $Zr_{36}Ti_{14}Cu_{12.5}Ni_5Be_{20.5}Fe_{12}$ composite.

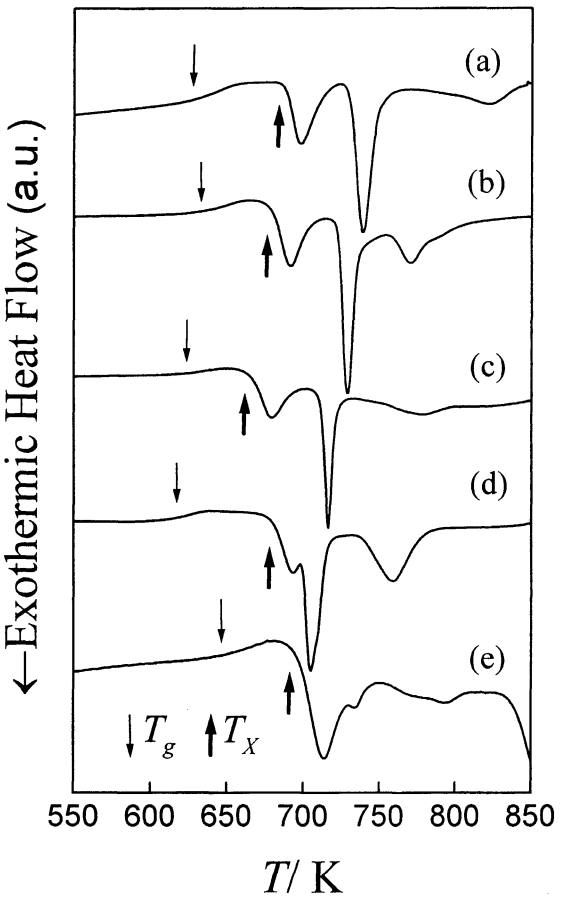

Fig. 3 DSC traces obtained from the $Zr_{41-X}Ti_{14}Cu_{12.5}Ni_{10-Y}Be_{22.5}Fe_{X+Y}$ alloys. (a) $X = Y = 0$; (b) $X = 0$, $Y = 2$; (c) $X = 0$, $Y = 5$; (d) $X = 0$, $Y = 8$; (e) $X = 5$, $Y = 0$.

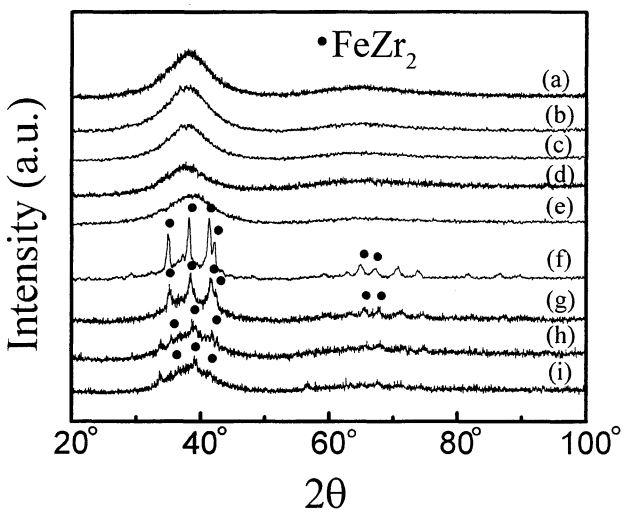

Fig. 1 XRD patterns for the $Zr_{41-X}Ti_{14}Cu_{12.5}Ni_{10-Y}Be_{22.5-Z}Fe_{X+Y+Z}$ alloys. (a) $X = Y = Z = 0$; (b) $X = Z = 0$, $Y = 2$; (c) $X = Z = 0$, $Y = 5$; (d) $X = Z = 0$, $Y = 8$; (e) $X = 5$, $Y = Z = 0$; (f) $X = Z = 0$, $Y = 10$; (g) $X = Y = 5$, $Z = 2$; (h) $X = Y = Z = 5$; (i) $X = Z = 5$, $Y = 8$.

have a wide SLR. The thermodynamic parameters of T_g, T_{x1}, ΔT, T_m, T_{rg}, ΔH_x (crystallization enthalpy) and ΔH_m (melting enthalpy) of the Zr–Ti–Cu–Ni–Be–Fe alloys are listed in Table 1. The value of T_g for these BMGs is not significantly affected by Fe addition. However, the T_{x1} and ΔT depend strongly on Fe content. The position and shape of the DSC exothermic peaks also change with the different Fe contents. The third crystallization peak disappears with increasing Fe content. The phenomena indicate that Fe addition leads to markedly different crystallization behaviors. The crystallization enthalpy of alloys increases greatly from 109.0 J/g to 158.8 J/g with increasing Fe content. The result means that the crystallization driving force is increased with increasing Fe addition. Figures 4(a)–(b) presents the changes of the T_{rg}, T_x, T_g and ΔT of the $Zr_{41}Ti_{14}Cu_{12.5}Ni_{10-X}Be_{22.5}Fe_X$ ($X = 0$, 2, 5, 8) alloys with Fe content. According to the theory of Turnbull,[11] if $T_g/T_m > 2/3$, homogeneous nucleation rate of an alloy will become extremely slow in the SLR, and the bulk metallic glass can be obtained. All the values of T_{rg} of the Fe bearing BMGs are greater than 2/3 confirming the excellent GFA of the alloys. Figure 4(b) shows that the T_g is almost unchanged with increasing Fe content. However, the T_x is very sensitive to the Fe addition. The alloy with 8 at%Fe has higher thermal stability. The Vicker Hardness (HV) versus Fe content of BMGs is shown in Fig. 5. Usually the compositional dependence of hardness is very weak in amorphous alloys with a single amorphous phase. In our case, 2 at%Fe addition can enhance the HV of the BMG, however, the HV decreases with increasing Fe content. The precipitation of the crystalline phase $FeZr_2$ reduces the value of HV, this phenomenon is different from that of the carbon and tungsten-bearing BMGs. Carbon and tungsten additions can greatly enhance the HV of the BMGs.[9,17] At present, we can not explain the phenomenon, and more work and study will be done to elucidate the interesting question.

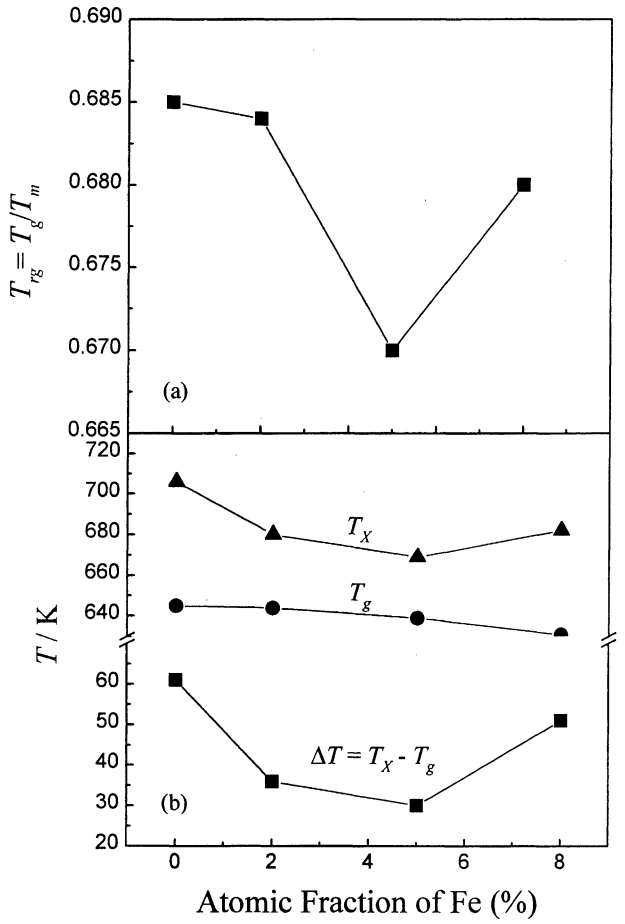

Fig. 4 The reduced glass transition temperature T_{rg} (a), the first crystalline temperature T_x, the glass transition temperature T_g and supercooled liquid region ΔT (b) for the $Zr_{41}Ti_{14}Cu_{12.5}Ni_{10-X}Be_{22.5}Fe_X$ ($X = 0$, 2, 5, 8) BMGs.

The magnetic susceptibility (χ) of the BMGs was measured at the range from 300 K to 800 K. Figure 6 exhibits the temperature dependence of χ at various Fe content. Each curve can be divided into three parts as indicated in Fig. 6. The first part ranges from 300 K to T_A. The amorphous structure of the alloy is not changed in this temperature range. The third part is from T_B to 800 K, the BMGs crystallize in the temperature range. The relation of χ upon temperature in the two parts can be expressed as follows:[18]

$$\chi = \frac{N P_{\text{eff}}^2 \mu_B^2}{3k} \times \frac{1}{T} + N\bar{\alpha} \qquad (1)$$

where, N is the number of the atoms, k is the Bolziman constant, P_{eff} is the effective magnetic moment for the low frequency of the atoms, μ_B is the Bore magneton, $\bar{\alpha}$ is the totality of the diamagnetic part and the high frequency part, which is independent of temperature. The plots of χ vs. $1/T$ for the BMGs are shown in inset of Fig. 6. The slopes of χ in the third part (corresponding to the crystallized state of the BMGs) are much larger than that of the first part (corresponding to the amorphous state of the BMGs). The values of P_{eff} for the crystallized BMGs are higher than that of the BMGs. However, the values of P_{eff} of Fe and Ni in liquid state[18] (the amorphous state is similar to undercooled liquid in structure and some properties) are higher than that of crystalline Fe and Ni. The curve of χ in the two parts also follows the law

Table 1 T_g, T_{x1}, ΔH_x, T_m, ΔH_m and T_{rg} (T_g/T_m) of the $Zr_{41-X}Ti_{14}Cu_{12.5}Ni_{10-Y}Be_{22.5}Fe_{X+Y}$ metallic glasses.

Samples	Structure	T_g (K)	T_{x1} (K)	ΔT (K)	ΔH_x (J/g)	T_m (K)	ΔH_m (J/g)	T_{rg}
$X = Y = 0$	A	645	706	61	109.0	941	125.3	0.68
$X = 0, Y = 2$	A	644	680	36	118.2	941	144.8	0.68
$X = 0, Y = 5$	A	639	669	30	116.2	954	146.5	0.67
$X = 0, Y = 8$	A	631	682	51	129.6	928	106.7	0.68
$X = 5, Y = 0$	A	649	703	54	158.8	938	89.7	0.69

Note: A stands for fully amorphous structure.

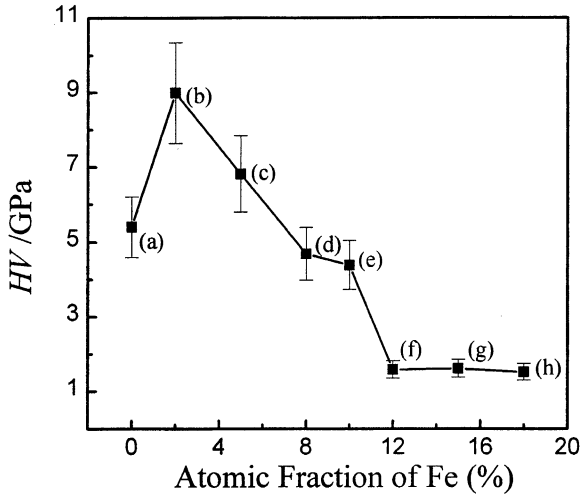

Fig. 5 Relationship of micro-hardness of the $Zr_{41-X}Ti_{14}Cu_{12.5}Ni_{10-Y}Be_{22.5-Z}Fe_{X+Y+Z}$ alloys upon composition. (a) $X = Y = Z = 0$; (b) $X = Z = 0$, $Y = 2$; (c) $X = Z = 0$, $Y = 5$; (d) $X = Z = 0$, $Y = 8$; (e) $X = 5$, $Y = Z = 0$; (f) $X = Z = 0$, $Y = 10$; (g) $X = Y = 5$, $Z = 2$; (h) $X = Y = Z = 5$; (i) $X = Z = 5$, $Y = 8$.

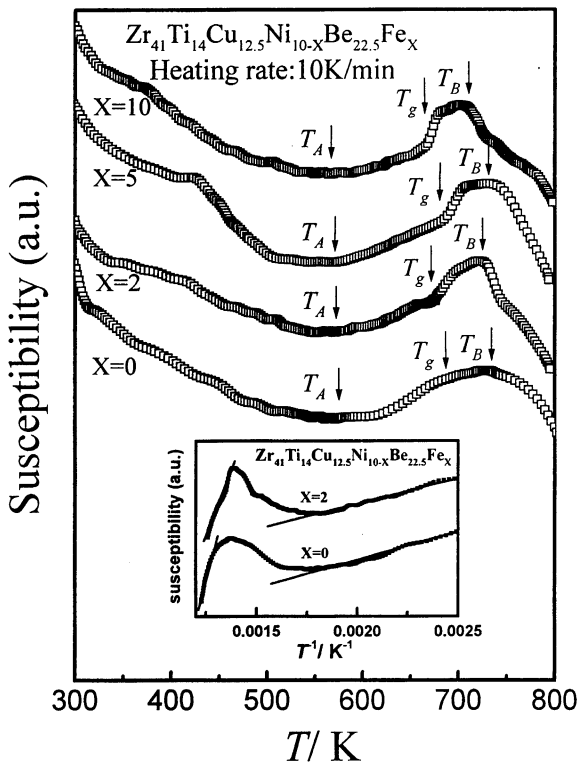

Fig. 6 Temperature dependence of the magnetic susceptibility upon temperature for the $Zr_{41}Ti_{14}Cu_{12.5}Ni_{10-X}Be_{22.5}Fe_X$ alloys ($X = 0, 2, 5, 10$). The insert shows the fits of the curves to the law of Curie-Weiss.

of Curie-Weiss.[18] The result indicates that the temperature-dependent change of χ follows the law of Curie-Weiss both in amorphous and crystalline states, which indicates that the amorphous and crystallized alloys are of paramagnetic property. The second part corresponds to the transitional region, the region from T_g to T_B is just corresponds to the SLR. Two remarkable χ change characteristics in this region should be noted: A sudden χ increase near T_g for the Fe-bearing BMG

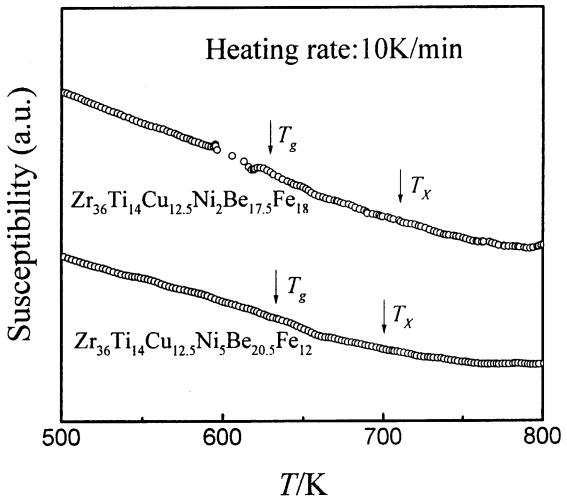

Fig. 7 Temperature dependence of the magnetic susceptibility for the $Zr_{36}Ti_{14}Cu_{12.5}Ni_2Be_{17.5}Fe_{18}$ and $Zr_{36}Ti_{14}Cu_{12.5}Ni_5Be_{20.5}Fe_{12}$ composites.

can be clearly seen. This result may indicate that the glass transition of the BMGs has the character of the second-order phase transition. In the SLR, χ increases with increasing temperature. The anomalous changes in the SLR of the Fe bearing BMGs indicate unique microstructural characteristics and properties of the SLR. The different temperature dependent behaviors of the Fe-bearing and Fe-free BMGs can be clearly seen in the inset of the figure. Figure 7 shows the magnetic susceptibility change upon temperature of the composites consisting of nanocrystalline particles. There is no anomalous change in the SLR and near T_g, even though the composites contain high Fe content. The curves fit well to the law of Curie-Weiss from room temperature to 800 K meaning paramagnetic properties. The results indicate that Fe itself is not responsible for the anomalous χ change in the BMG, the glass transition and special structure of the supercooled liquid of the Fe-bearing BMGs cause the changes. The origin of the phenomenon needs to be clarified in future.

4. Conclusions

$Zr_{41}Ti_{14}Cu_{12.5}Ni_{10-X}Be_{22.5}Fe_X$ ($X = 0, 2, 5, 8$) BMGs were fabricated by water quenching method. It was found that the GFA, crystallization behaviors and the properties of the alloys were sensitive to Fe content. Fe addition resulted in a decrease of GFA and thermal stability. The composites consisting of $FeZr_2$ nanocrystalline particles embedded in the glassy matrix were obtained in the alloy with more than 10 at%Fe addition. These fully BMGs exhibited high thermal stability, wide super-cooled liquid region and high Vicker's hardness. An anomalous changes of the magnetic susceptibility versus temperature, which may results from the unique microstructural characteristic, was observed for the Fe contented BMGs in the SLR.

Acknowledgement

We are grateful to the financial support of the National

Natural Science Foundation of China (Grant number: 59925101, 59871059)

REFERENCES

1) A. Peker and W. L. Johnson: Appl. Phys. Lett., **63** (1993), 2342–2344.
2) A. Inoue, N. Nishiyama and T. Matsuds: Mater. Trans., JIM, **37** (1996), 181–184.
3) R. Raicheff, V. Zaprianova and E. Gattef: J. Mater. Sci. Lett., **16** (1997), 1701–1703.
4) X. Y. Zhang, J. W. Zhang, R. P. Liu, J. H. Zhao and Y. Z. Zheng: J. Mag. Mag. Mater, **172** (1997), 301–307.
5) J. Zbroszczyk: Journal de Physique I, **7** (1997), 1019–1023.
6) W. L. Johnson: Mater. Sci. Forum, **225–227** (1996), 35–47.
7) A. Inoue, T. Zhang and A. Takeuchi: Appl. Phys. Lett., **71** (1997), 464–466.
8) A. Inoue, A. Murakami, T. Zhang and A. Takeuchi: Mater. Trans., JIM, **38** (1997), 189–196.
9) W. H. Wang, Q. Wei and S. Friedrich: Phys. Rev. B, **57** (1998), 8211–8217.
10) W. H. Wang, Q. Wei and H. Y. Bai: Appl. Phys. Lett., **71** (1997), 58–60.
11) W. H. Wang, Q. Wei, S. Friedrich and H. Wollenberger: Appl. Phys. Lett., **71** (1997), 1053–1055.
12) A. Gebert, J. Eckert and L. Schultz: Mater. Sci. Forum, **269–272** (1998), 797–801.
13) W. H. Wang, R. J. Wang, D. Q. Zhao and M. X. Pan: Appl. Phys. Lett., **74** (1999), 1803–1805.
14) H. Choi-Yim, R. Busch and W. L. Johnson: J. Appl. Phys., **83** (1998), 7993–7997.
15) C. Fan, A. Takeuchi and A. Inoue: Mater. Trans., JIM, **40** (1999), 42–51.
16) A. R. Miedema and A. K. Niessen: *Cohesion in Metals*, North-Holland Publishing Company, (1988), pp. 68–71.
17) H. Choi and W. L. Johnson: Appl. Phys. Lett., **71** (1997), 3808–3810.
18) D. S. Dai and K. M. Qian: *Ferromagnetism*, Chinese Scientific Publication, (1992), pp. 29–70.
19) R. Wang: Nature, **278** No. 5706 (1979), 700–704.